

Research Paper

A response factor approach to modelling long-term thermal behaviour of energy piles

Simon Rees^{a,*}, Gust Van Lysebetten^b

^a University of Leeds, School of Civil Engineering, Woodhouse Lane, Leeds LS2 9JT, United Kingdom

^b Belgian Building Research Institute (BBRI), Avenue P. Holoffe 21, B1342 Limelette, Belgium

ARTICLE INFO

Keywords:

Geothermal energy
Ground heat exchanger
Energy pile
Thermal performance
Model validation

ABSTRACT

Predicting the long-term thermal performance of an energy pile ground heat exchanger system requires a computationally efficient model that captures the three-dimensional features and interacting thermal boundary conditions found in such systems. We present a model that employs a response factor approach to predicting long-term thermal behaviour based on a Dynamic Thermal Network representation. This allows fully three-dimensional geometric representation of the problem and application of boundary conditions at the ground and building sub-surfaces in addition to the pipes. The model has been validated using data from long-term monitoring of a pile in Belgium excited by a combination of heating and cooling demands in a range of environmental conditions. We further demonstrate application of the model to simulated annual building energy demands and the significance of treatment of the upper surface boundary conditions. The model is shown to be capable of representing building system and environmental conditions effectively and furthermore computationally efficient enough for routine design and simulation tasks.

1. Introduction

Heating and cooling systems that rely on heat pumps and some form of ground heat exchanger are one of the most effective means to implementing energy efficient building thermal systems and addressing the need for carbon emissions reduction [1–3]. Of the various types of ground heat exchanger that are in use, making use of building sub-structure (foundation) elements is one of the most attractive options: particularly for larger non-residential buildings [4,5]. A number of types of sub-structural building elements have been used as the basis of ground heat exchangers, including piles, diaphragm walls and ground-coupled slabs. One of the most common forms used for heat exchange are so called Energy Piles [6]. Energy pile technology has been applied to a number of non-residential building types, including airports [7], institutional buildings [8], retail developments [9], office buildings [10] and stations [6]. Modelling of the thermal performance of this form of ground heat exchanger is the subject of this paper.

In contrast to research in the well established and widely applied borehole and shallow horizontal ground heat exchanger technologies, this research effort has been motivated by geotechnical concerns as much as those of heating and cooling system design. Examination of theoretical and lab-scale studies of the variation of fundamental properties of soils induced by temperature variations naturally leads to

concerns over the reduction in the mechanical performance of thermally activated piles compared to thermally passive designs [11]. The issues to be considered are chiefly [12] thermally induced: (i) vertical displacements, (ii) stresses within the pile, and (iii) changes in load resistance. Analysis and modelling efforts have consequently often focussed on Thermo-Hydraulic-Mechanical (THM) coupled models able to deal with the complexities of the coupled soil-structure interactions under particular thermal conditions [13].

The use of THM models for energy pile studies raises the question as to what thermal boundary conditions (i.e. heat fluxes and fluid temperatures imposed by the building system and climatic conditions) are to be used to assess geotechnical design risk (e.g. load bearing capacity and allowable displacements) when applying such models. In general, the computational efficiency of THM models (typically 3D Finite Element formulations) means that they are not well suited to answering this question themselves. This is because understanding the range of likely thermal conditions requires application of time-varying building heating and cooling demands (e.g. hourly variations) over very long timescales. Typically twenty or twenty-five years of simulation time are required before a geothermal heat exchange system can be shown to reach a steady-periodic state indicative of the sustainability of a design [14]. As system heat loads are not dependent on mechanical conditions, the task of modelling the effect of thermal boundary conditions and

* Corresponding author.

E-mail address: S.J.Rees@leeds.ac.uk (S. Rees).

Nomenclature

C	specific heat capacity, $\text{kJ kg}^{-1} \text{K}^{-1}$
h	heat transfer coefficient, $\text{W m}^{-2} \text{K}$
K	conductance, W K^{-1}
\bar{K}	modified conductance, W K^{-1}
n	normal to the boundary, –
N	number of surfaces
Q	heat transfer rate, W
\bar{Q}	average heat transfer rate, W
r	pipe radius, m
R	thermal resistance, $\text{K m}^2 \text{W}^{-1}$
S	surface area, m^2
t	time, s
Δt	time step size, s
T	temperature, $^{\circ}\text{C}$
\bar{T}	weighted average temperature, $^{\circ}\text{C}$

Greek symbols

α	thermal diffusivity, $\text{m}^2 \text{s}^{-1}$
ε	heat exchanger effectiveness, –
ω, φ, ψ	time step, s
κ	weighting function
λ	thermal conductivity, $\text{W m}^{-1} \text{K}^{-1}$
ρ	density, kg m^{-3}
τ	time (integration variable), s
θ	hourly time variable, h

Subscripts

i, j	surface number
n	time step index
a	admittive
t	transmittive
ρ	weighting factor index

heat transfer rates can be dealt with separately using tools concerned only with conduction heat transfer as we do here. This is reasonable as long as changes in mechanical conditions during normal operation of the building have only a secondary effect on thermal properties.

An important consideration regarding thermal conditions imposed at the surfaces surrounding an energy pile installation are those related to the building basement or slab elements covering the piles. The presence of the building, and the fact that it is maintained at something approximating room temperature during its life, mean that heat is continually rejected into the ground after the start of operations. Consequently, there are differential surface conditions to consider: outside the building where the ground is exposed to solar irradiation and precipitation, and under the building where there is isolation from such effects but continual heating of the ground. We investigate the significance of such effects later in this paper.

It is often the case that the overall heat exchange capabilities of a building's energy pile system have to be supplemented by more conventional heat exchanger devices such as air coolers in a hybrid configuration [9,15]. Design of hybrid systems is dependent on being able to predict the time-varying fluid temperatures at hourly or sub-hourly time steps and over multi-year periods. This tends to preclude direct application of three-dimensional numerical models. Where such models have been applied over long timescales, this has required simplification of the load profile (e.g. to annual sinusoidal form) so that very large time steps can be used [16,17].

Widely adopted approaches to the thermal design and simulation of ground heat exchange systems of the borehole type, are to apply reduced order or response factor methods. Reduced order approaches include one or two-dimensional numerical models and lumped capacitance–resistance networks. This approach has been applied in analysis of energy piles for single piles only but has the advantage of dealing with the short timescale effects in the fluid [18]. A hybrid of these approaches is used in the PILESIM software [19] which evolved from an earlier model of borehole thermal energy storage systems [20].

The approaches that can be classified as response factor methods all rely on spatial and temporal superposition of responses to some form of heat flux or temperature pulse. This can be applied by decomposing the time series of imposed heat fluxes into an equivalent series of pulses or steps. The definition of unit heat flux step pulse responses in so-called 'g-functions' [14] has also been applied to energy pile design calculations [21,22]. This formulation of the responses for long timescales has the advantage of being possible to quantify response in non-dimensional form for a given pile aspect ratio and array configuration i.e. independent of ground thermal conductivity [22]. Shorter time scales, where heat exchange occurs mostly within the pile boundary, can be

dealt with by a slightly different approach depending on the two-dimensional layout of pipes within the pile [21]. Hence a pile array response is defined by a combination of short and long timescale g-functions.

Both reduced order and response factor approaches satisfy the need for simulations that are efficient at short time steps and multi-year simulation. However, they generally assume heterogeneous thermal properties and only consider time-varying boundary conditions at the pipe and simple initial conditions i.e. uniform temperature. Hence this does not allow consideration of initial ground temperature gradients or differentiate between ground and sub-structure boundary temperatures.

A further approach that seeks to reduce the order of the thermal analysis problem to one that is computationally efficient has been developed by Makasis et al. [23,24]. This approach linearizes the response of fluid temperature to changes in applied heat flux through application of a fully three-dimensional Finite Element model to simulate a response to large heat pulses over long timescales (a number of years). The linear response parameters for a particular configuration are derived from the final year of the simulation. These response parameters are further analysed for a large number of cases so that correlations can be derived according to design parameters such as heat exchanger dimensions. This approach can be applied to a range of ground heat exchanger types e.g both piles and diaphragm walls. This seems to assume the systems are isolated from the ground surface and that short pulses of heat flux respond the same way as long.

2. Model development

The aim in developing a model of energy pile thermal response is to be able to make studies of both short and long-term thermal performance with high computational efficiency. This implies being able to simulate conditions with time varying inlet fluid temperatures and flow rates that fluctuate over hourly or sub-hourly time scales for simulations over several years i.e. tens of thousands of time steps. This precludes using conventional numerical approaches such as Finite Volume or Finite Element modelling. Accordingly, we have sought to apply an approach that falls into the category of response factor methods. Simulation at short time scales and accurate prediction of fluid temperature fluctuations is important to assessment of heat pump and hence overall system efficiency.

Further to the discussion of the influence of the ground surface and building sub-surface conditions, we have the further objective of applying a method that can deal with time varying boundary conditions applied at three surfaces and that it is able to deal with three-dimensional geometric effects. The three boundaries of interest in this

application are defined at the pipe, ground and building surfaces. The Dynamic Thermal Network approach we have applied also has the advantage that heterogeneous ground properties can be applied. The basis of the method is summarized below; further details are available in reports of earlier work [25,26].

2.1. Dynamic thermal network representation

The concept of representing heat transfer as a network of nodal temperatures and resistances is extended in the Dynamic Thermal Network (DTN) approach to deal with transient conduction in heterogeneous solid bodies where the heat fluxes are driven by time varying boundary temperatures. The concept and the underlying mathematical principles were developed by Claesson [27–29] and Wentzel [30] with application to building structures and components in mind i.e. solid bodies that have considerable thermal capacity and require simulation over long time scales.

The heat conduction problem in this context can be formulated according to Fourier’s Law with constant properties and a set of N boundary conditions of the mixed type with constant surface heat transfer coefficients, h ,

$$\nabla \cdot (\lambda \nabla T) = \rho c \cdot \frac{\partial T}{\partial t} \tag{1}$$

$$h_i \cdot [T_i(t) - T_{s_i}] = \lambda \cdot \frac{\partial T}{\partial n}, \quad [i = 1 \dots N]$$

In this form of conduction problem, the primary interest is in the relationship between boundary fluxes and temperatures rather than internal body temperatures. Once the differential equation has been solved to find the temperatures, the boundary heat fluxes of interest associated with surface i of area S_i , can be calculated using,

$$Q_i(t) = S_i \cdot h_i \cdot [T_i(t) - T_{s_i}] \tag{2}$$

In general, the network may include any number of surfaces but most problems of interest have two or three surfaces. The network representation of a three-surface problem is illustrated in Fig. 1. One of the essential features of the DTN method is that heat fluxes at each surface are separated into admittive and transmittive components. Admittive fluxes are associated with variations in temperature at that boundary. In the case of an adiabatic surface, the only fluxes are those brought about by variations in temperatures at that surface. Where there is heat transfer at another surface, an additional component is superimposed depending on the difference between the boundary temperatures: this is the transmittive component. In general both components of the heat flux are present. In the network model diagram, a single ended heat transfer path is associated with each node to represent the admittive heat transfer path. The reversed summation symbols (Σ) adjacent these conductances in Fig. 1 indicate driving temperatures that are averages of the current and previous temperatures. In the single ended admittive path, the single summation sign indicates the driving temperature is a function of the average temperature at that boundary alone.

Another feature of the DTN approach is that the temperatures, $T_i(t)$, and fluxes, $Q_i(t)$, of the dynamic network are defined at boundary temperature nodes rather than at the surfaces themselves. These boundary temperatures are typically the air temperature but can be defined in a modified form to deal with more complex thermal boundary conditions. We accordingly make a distinction between the terms ‘boundary’ and ‘surface’ in the following discussion. There is a constant conductance defining the instantaneous heat transfer between the boundary and the surface itself: $S_i \cdot h_i$ in Eq. (2).

For a model of an energy pile ground heat exchanger we define three surfaces at which different time-varying boundary conditions are applied. It is sufficient to represent the pipe system as a single boundary surface. Although in deeper ground heat exchanger systems such as

borehole heat exchangers the ground is regarded as a constant temperature boundary condition, for this application the ground is thought to have a more significant influence on thermal conditions—at least at longer time scales—and so we define this as a further boundary at which time-varying conditions can be applied. The other boundary of interest is that where the head of the pile is exposed to thermal conditions governed by the associated building: the building generally having an insulating or heating effect over the long term. This might be defined under a ground bearing slab or sub-surface space. This concept is illustrated in Fig. 2.

The conductances in the admittive path of the network are denoted with a single subscript K_i and are equal to the surface area multiplied by a constant heat transfer coefficient, e.g., $K_i = S_i \cdot h_i$. There are constant conductances between each pair of surfaces denoted with double subscripts K_{ij} along the transmittive path. These conductances are the overall steady-state conductances between the boundaries and include the surface conductances K_i and K_j . The nodal heat balance equations set out the relationship between the total flux at each boundary and the admittive and transmittive components. For a three-surface problem the heat balance equations are,

$$\begin{aligned} Q_1(t) &= Q_{1a}(t) + Q_{12}(t) + Q_{13}(t) \\ Q_2(t) &= Q_{2a}(t) + Q_{21}(t) + Q_{23}(t) \\ Q_3(t) &= Q_{3a}(t) + Q_{31}(t) + Q_{32}(t) \end{aligned} \tag{3}$$

where the ‘ia’ subscript denotes the time-varying admittive component of the flux and the ‘ij’ subscript denotes the transmitted component between pairs of boundaries.

Although the general DTN formulation does not rely on any particular form of excitation it is helpful to appreciate the relationship between the admittive and transmittive fluxes by considering application of a step change in boundary temperature at one of the surfaces. Consider the response for a energy pile with three boundaries defined as in Fig. 3. The response when a step change in boundary temperature is applied at the pipe surface (1) and the temperature at the ground and building surfaces (2 and 3) are held at zero. At the beginning of the step change, the flux at the pipe surface being excited (Q_1) is entirely admittive in nature and is limited by the surface conductance ($Q_1 = Q_{1a}$ at $t = 0$). As steady-state is approached ($t > 10^6$ in this case), the admittive component approaches zero and the transmittive flux to the other two surfaces approaches the steady-state value. At any time, the admittive component is given by the difference between the total flux and the sum of the transmittive fluxes with the other boundaries. The steady-state pipe flux can be seen to be balanced by the combination of building and ground fluxes in Fig. 3. The pipe flux can also be seen to be strongly sensitive to the admittive flux at short time scales (less than 10 h in this case). This is of some significance in energy pile systems in that it suggests, where fluxes vary on a daily basis, much of the heat transfer will be admittive i.e. to and from the concrete of the pile and less so with the surrounding ground.

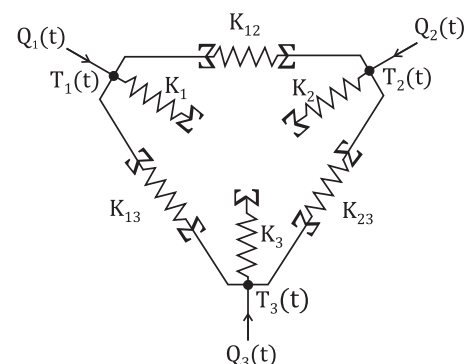


Fig. 1. The dynamic thermal network representation of a body with three boundaries (after Rees and Fan [25]).

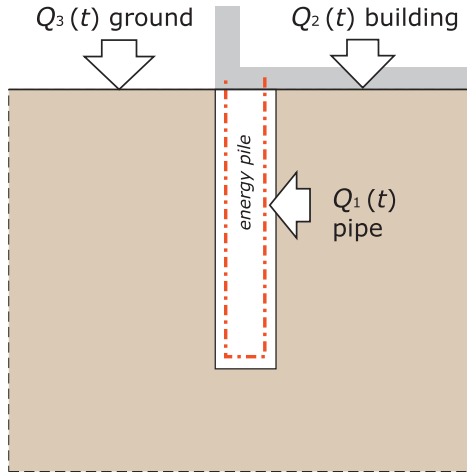


Fig. 2. Definition of the three boundary surfaces and corresponding time-varying heat fluxes in a DTN representation of a diaphragm wall ground heat exchanger.

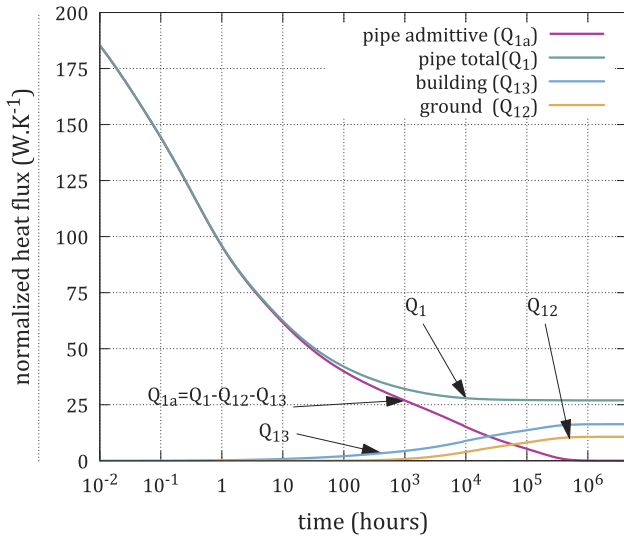


Fig. 3. Calculated fluxes for an energy pile with a unit step change in temperature at the pipe boundary. Note that time is shown on a logarithmic scale.

Claesson [28] showed that the temperature differences driving the absorptive and transmittive fluxes can be always defined in an exact manner by the current and weighted averages of the previous boundary temperatures. The absorptive and transmittive fluxes at a given boundary can be written in terms of the conductances and these temperatures as follows,

$$Q_{ia}(t) = K_i \left(T_i(t) - \int_0^\infty \kappa_{ia}(\tau) \cdot T_i(t - \tau) d\tau \right) \quad (4)$$

$$Q_{ij}(t) = K_{ij} \int_0^\infty \kappa_{ij}(\tau) \cdot [T_i(t - \tau) - T_j(t - \tau)] d\tau \quad (5)$$

These weighted average temperatures are those associated with the points in the network indicated by a reversed summation symbol (Fig. 1). The temperatures are averaged according to weighting functions, κ_{ia} and κ_{ij} for the admittive flux at the surface and the transmittive flux between surfaces respectively. A shorthand notation is used to denote these weighted average temperatures as follows,

$$\bar{T}_{ia}(t) = \int_0^\infty \kappa_{ia}(\tau) \cdot T_i(t - \tau) d\tau \quad (6)$$

$$\bar{T}_{ij}(t) = \int_0^\infty \kappa_{ij}(\tau) \cdot T_i(t - \tau) d\tau \quad (7)$$

Using this notation and substituting Eqs. (6) and (7) into Eq. (3) allows the heat balance equations for each surface to be expressed as,

$$\begin{aligned} Q_1(t) &= K_1 \cdot [T_1(t) - \bar{T}_{1a}(t)] + K_{12} \cdot [\bar{T}_{12}(t) - \bar{T}_{21}(t)] \\ &\quad + K_{13} \cdot [\bar{T}_{13}(t) - \bar{T}_{31}(t)] \\ Q_2(t) &= K_2 \cdot [T_2(t) - \bar{T}_{2a}(t)] + K_{12} \cdot [\bar{T}_{21}(t) - \bar{T}_{12}(t)] \\ &\quad + K_{23} \cdot [\bar{T}_{23}(t) - \bar{T}_{32}(t)] \\ Q_3(t) &= K_3 \cdot [T_3(t) - \bar{T}_{3a}(t)] + K_{13} \cdot [\bar{T}_{31}(t) - \bar{T}_{13}(t)] \\ &\quad + K_{23} \cdot [\bar{T}_{32}(t) - \bar{T}_{31}(t)] \end{aligned} \quad (8)$$

As the steady-state is approached, each average temperature approaches the related boundary temperature and the admittive fluxes become zero. In the steady-state Eq. (8) reduces to the usual expression for flux in terms of overall conductance and boundary temperatures ($Q_1 = K_{12} \cdot [T_1 - T_2] + K_{13} \cdot [T_1 - T_3]$, etc.).

2.2. Discretization

The required weighting functions can be found by applying the a unit step in boundary temperature at one of the surfaces and holding the other boundary temperatures at zero and repeating this for each boundary (as in Fig. 3). Claesson [28,29] showed that where the boundary temperatures vary in a piecewise linear fashion, the exact weighting factors can be obtained using the admittive and transmittive fluxes calculated from the step responses averaged over each step (size Δt). The discrete weighting factors are then obtained from the differences in these average time step fluxes as follows,

$$\begin{aligned} \kappa_{ia,\rho} &= \frac{\bar{Q}_{ia}(\varphi) - \bar{Q}_{ia}(\omega)}{\bar{K}_i} \\ \kappa_{ij,\rho} &= \frac{\bar{Q}_{ij}(\omega) - \bar{Q}_{ij}(\varphi)}{K_{ij}} \end{aligned} \quad (9)$$

where the time differences are between $\varphi = (\rho\Delta t - \Delta t)$ and $\omega = \rho\Delta t$. In the case of the admittive weighting factors a modified surface conductance (\bar{K}_i) defined that is equal to the initial admittive flux, $\bar{K}_i = \bar{Q}_{ia}(0)$.

When the boundary temperatures are defined by a discrete time series, the average temperatures are calculated by the summation of weighting factor sequences multiplied by boundary temperature sequences that represent the state at previous time steps. The discrete form of Eqs. (6) and (7) are, for current time step n ,

$$\bar{T}_{ia,n} = \sum_{\rho=1}^{\infty} \kappa_{ia,\rho} \cdot T_{i,n-\rho} \quad (10)$$

$$\bar{T}_{ij,n} = \sum_{\rho=0}^{\infty} \kappa_{ij,\rho} \cdot T_{i,n-\rho} \quad (11)$$

For a given set of boundary temperatures, the fluxes can then be calculated (i.e. in the process of a simulation) using Eq. (8). Updating the temperature histories can be done efficiently at each step and the heat balance equations are simple algebraic expressions. The result is that the overall computational efficiency of the simulation process is very efficient.

2.3. Boundary conditions

The DTN is formulated assuming that surface heat transfer coefficients (h) are constant. This is sufficient for some cases but often more complex thermal boundary conditions need to be implemented. The approach we have taken to implement more complex boundary conditions has been to define a boundary temperature that is an 'effective temperature' (T_e) such that, when applied using the predefined constant heat transfer coefficient, gives the expected surface heat flux as

applying a more complex boundary condition model. This effective temperature does not correspond directly to a physical boundary temperature but is applied in the DTN heat balance equations and when the weighted average temperature is updated. In this application we do this using slightly different formulations for the pipe, ground and building boundaries.

At surfaces exposed to the external environment, convection processes act in combination with short-wave and long-wave radiant fluxes. A surface heat balance defining such a boundary condition for this study is,

$$\frac{Q_i}{S_i} = R_{sw} + R_{lw} + h_{ca}(T_a - T_{Si}) \quad (12)$$

The effective boundary temperature is intended to give the equivalent heat flux and hence is defined by,

$$\frac{Q_i}{S_i} = h_i(T_e - T_{Si}) \quad (13)$$

Hence the equivalent boundary temperature must be,

$$T_e = [R_{sw} + R_{lw} + h_{ca}T_a + (h_{ca} - h_i)T_{Si}]/h_i \quad (14)$$

At the building sub-surface, a reduced form of this expression that ignores solar and longwave radiation is all that is necessary.

In geometries with embedded pipes like a diaphragm wall, it is necessary to define the relationship between the boundary temperature and both the pipe fluid inlet and outlet temperatures. Our approach is—similar to that of Strand [31]—to assume the pipe surface temperature does not vary along its length and make an analogy with an evaporating-condensing heat exchanger and so to define a characteristic effectiveness parameter (ϵ). The pipe fluid heat balance is then defined by the maximum possible temperature difference and the effectiveness as follows,

$$Q_p(t) = \epsilon \dot{m}C(T_{in}(t) - T_p(t)) \quad (15)$$

For such a heat exchanger,

$$\epsilon = 1 - e^{-NTU} \quad (16)$$

and this is related to the total pipe area and fluid heat transfer coefficient by the Number of Transfer Units (NTU) as follows,

$$NTU = \frac{2\pi rH \cdot h_p}{\dot{m}C} \quad (17)$$

In the implementation of the energy pile model, we use the outside of the pipe (i.e. the concrete cylindrical surface) as the boundary and calculate an equivalent heat transfer coefficient (h_x) to take account of the fluid and pipe material thermal resistances. We have chosen to calculate fluid convective heat transfer using the well known correlation by Gnielinski [32] along with the explicit approximation by Serghides [33] to find the friction factor. The Gnielinski correlation is valid to relatively low Reynolds Numbers but to deal with the transitional regime some interpolation between this function and the laminar value is required.

It is possible, by rearranging the heat balance equations to calculate the effective pipe boundary temperature in a way that avoids iteration using only the inlet temperature (T_{in}) as the time-varying input data as follows. The temperature that needs to be defined in the DTN heat balance equation for the pipe in this case is T_1 at a given time step. An instantaneous heat balance can be defined at the pipe surface by equating Q_p (Eq. (15)) with the convective flux at the surface (dropping the t for simplicity) as follows,

$$\epsilon \dot{m}C(T_{in} - T_p) - h_x S_1(T_1 - T_p) = 0 \quad (18)$$

A further heat balance can be defined using the DTN heat balance equation for surface 1 (Q_1 in Eq. (8)) and the convective flux,

$$K_1[T_1 - \bar{T}_{1a}] + Q_{12} + Q_{13} - h_x S_1(T_1 - T_p) = 0 \quad (19)$$

The term with \bar{T}_{1a} is based on past temperatures and so is known at the start of any time step. As the transmittive fluxes change very slowly, these can also be taken as the most recently calculated values. Accordingly these can be grouped into a term \bar{Q} representing the historical fluxes so that the heat balance can be abbreviated to,

$$K_1 T_1 + \bar{Q} - h_x S_1(T_1 - T_p) = 0 \quad (20)$$

This can be rearranged to find an expression for T_p ,

$$T_p = T_1 - \frac{K_1 T_1 + \bar{Q}}{h_x S_1} \quad (21)$$

This can be substituted in Eq. (18) to eliminate T_p . This gives an expressions for T_1 that only involves the inlet temperature and historical heat fluxes as follows,

$$T_1 = (T_{in} - \bar{Q}/h_x S_1) / \left(1 - \frac{K_1}{h_x S_1} + \frac{K_1}{\epsilon \dot{m}C}\right) \quad (22)$$

The outlet temperature can then be found from the fluid heat balance as follows

$$T_{out} = T_{in} - Q_p/\dot{m}C \quad (23)$$

2.4. Derivation of discrete weighting factors

Derivation of the weighting factors for the DTN method is most conveniently done by analysis of step responses at each boundary in turn. The values of the fluxes resulting from the step change depend on the geometry and thermal properties of the problem being considered and it is not necessary to assume homogeneous properties. The method used to calculate the step response can vary: both analytical and numerical methods have been used in other applications. In this case we use a numerical model for this task. To make this efficient, we have implemented a parametric method of mesh generation for arrays of energy piles and have used the OpenFOAM library [34] to calculate conduction heat transfer over the whole range of timescales. The solver was adapted to use increasing time steps to make the process efficient. The parametric mesh generation tool generates the required geometry and mesh definition given basic design parameters (pipe and pile diameter, depth, pipe pitch diameter etc.). An example of an energy pile mesh for a single pile is shown in a horizontal cross-section in Fig. 4.

Having generated three sets of response data in the form of heat flux time series (as in the example shown in Fig. 3), discrete weighting factors are calculated for the chosen time step size using Eq. (9). The details of this process and how the weighting factors are reduced to a compact data set, are described by Wentzel [30] and in Rees and Fan [25]. An illustration of the weighting factor series for the admittive flux

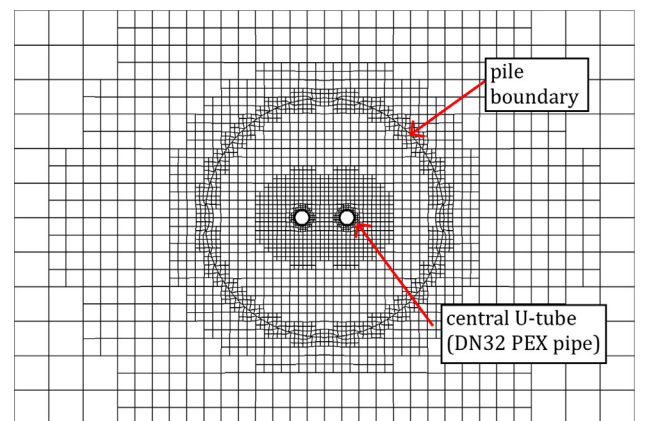


Fig. 4. A parametrically generated numerical mesh of an energy pile shown in a horizontal cross-section. This configuration corresponds to that used in the validation study.

of an energy pile are shown in Fig. 5.

2.5. The modelling process

The application of the DTN method described here can be thought of as a process in two stages. As the weighting factors only need to be calculated once, they can be stored for later/repeated use. Weighting factors are calculated for each combination of geometry and thermal properties for a given class of problem. The steps required for the generation stage (G1–G5) can be summarized as follows:

- G1. parametric generation of a numerical mesh based on geometric design parameters and particular thermal properties;
- G2. numerical step-response calculations for each surface using variable time steps;
- G3. analysis of step response data to derive discrete weighting factor series;
- G4. application of a weighting factor reduction procedure;
- G5. storage of the weighting factor data.

A library of weighting factor data can be built-up for application is design and system modelling tools as needed. The simulation process itself is implemented separately. The simple nature of the heat balance equations and the shifting of data in the temperature update process mean that long time series can be processed very efficiently. The simulation steps (S1–S4) can be summarized as:

- S1. initialisation of the weighting factor data, discrete temperature data and calculation of the initial mean temperatures,
- S2. calculation of the surface heat fluxes using time-varying boundary conditions (Eq. 3);
- S3. updating the mean temperature data series (Eq. 11);
- S4. calculation of model output temperatures and heat transfer rates.

The steps S2–S4 are repeated to the end of the boundary condition time series.

3. Energy pile testing and monitoring

We have sought to validate the model using data from a full size pile under a range of thermal excitation conditions: both heating and cooling. The approach to validation has been to use the measured inlet temperatures and flow rates as boundary conditions to the model and compare the predicted and measured outlet temperatures and heat transfer rates.

3.1. Energy pile testing installation

The energy pile used in the validation study is part of an energy pile test field in Ostend, Belgium, consisting of 5 energy piles with a length of 11.5 m [35]. These piles were installed for long-term thermal and thermo-mechanical testing purposes. Mechanical and steady-state thermal data were reported and discussed previously [35]. Allani et al. [36] discuss the validation of a finite element model of thermo-mechanical energy pile behaviour based on the monitoring data of the same pile as used in this validation study. In the study reported here, the temperature and flow rate data that define the dynamic performance over the whole experimental monitoring programme have been used. The heads of the piles and the adjacent ground surface was exposed to the environment during the test series i.e. no building over the piles was present.

3.2. Pile and ground characterisation

The energy pile from which data is used for model validation, is a

soil displacement screw pile with screw shaped shaft (360/560 mm). A single U-loop heat exchanger (PE-Xa 32 × 2.9 mm pipe) has been mounted on the reinforcement cage before installation, together with 2 small diameter hollow steel tubes for instrumentation purposes after pile installation.

The soil stratigraphy of the test site has been characterized based on Cone Penetration Test (CPT) data and analysis of drilling samples (Table 1). Thermal conductivity properties of the pile concrete and undisturbed soil samples as determined in laboratory (respectively with a half-space needle probe and a needle probe) are summarized in Table 2. In the validation study the weighting factors have been calculated after applying the thermal properties of the respective layers. It has not been necessary to assume heterogeneity as in other response factor approaches. Thermal property values for the pile are weighted to account for the presence of the reinforcement. Note that groundwater levels were high but movement of groundwater is not considered explicitly in this model.

3.3. Thermal excitation and monitoring

The fluid temperature was monitored at inlet and outlet of the pile and at different levels inside the U-loop heat exchanger using type T thermocouples. Soil temperature near the piles was measured as well at several depths and distances to the piles. This has enabled the vertical temperature gradient to be evaluated. At the start of the test series the temperature at 10 m depth was 14.1 °C. For part of the test campaign the external dry-bulb temperature was also measured. We have supplemented this data with that from local weather station records.

The energy piles are thermally excited through a hydronic thermal system that allows heating and cooling of the piles at a constant temperature at the inlet between −4 °C and +40 °C. The system is also designed to supply a constant temperature difference (heat transfer rate) between heat exchanger inlet and outlet (e.g. to perform a thermal response test).

The flow rate and temperature data over the whole of the test series are illustrated in Fig. 6 along with the atmospheric dry-bulb temperature. The total duration of the test series is 16 June 2015 to 9 February 2016 with data recorded at minutely intervals. We have denoted different periods of the test campaign according to phases 1–4 for the purposes of the discussion below. There was a gap in recording of the data between the end of phase 1 and start of phase 2 when no thermal testing took place. As we have investigated the effect of the

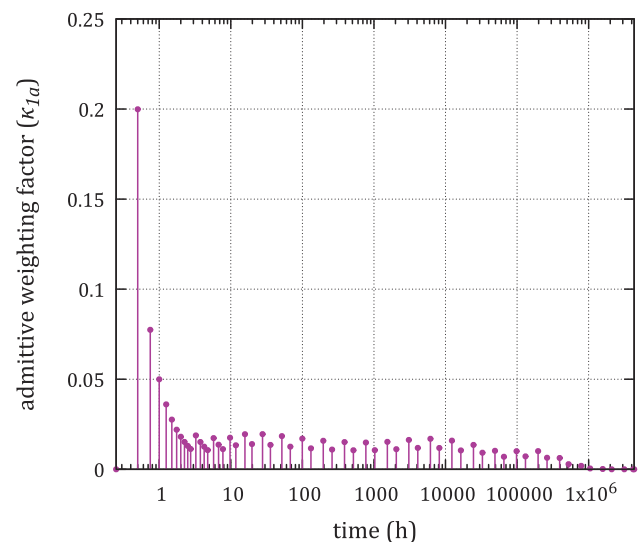


Fig. 5. An example of a discrete weighting factor data series for the admittive flux ($\kappa_{I,a}$) at an energy pile pipe boundary. The time intervals can be seen to double as time increases and magnitude decreases.

Table 1
Ground material layers at the pile test site.

Depths	Material
0–5 m	soft clay, locally organic
5–6 m	very soft peat
6–10 m	dense sand
10–11 m	very soft clay
11–12 m	dense sand
12–12.5 m	soft clay
12.5–14 m	dense sand
14–16 m	soft clay

Table 2
Ground material and pile thermal properties at the pile test site.

Property	Units	Clay	Peat	Sand	Pile
Specific heat (c_s)	$\text{kJ kg}^{-1} \text{K}^{-1}$	1000	850	1000	806
Thermal conductivity (λ)	$\text{W m}^{-1} \text{K}^{-1}$	1.5	1.5	2.0	2.84
Density (ρ)	kg m^{-3}	2500	2200	2500	2500

environmental boundary conditions in this study, we have completed this part of the data series with the corresponding environmental data (dry-bulb, relative humidity, global solar irradiation and wind speed) from the Ostend weather data record. The whole test series is treated as a continuous data series in the validation calculations i.e. all phases were simulated together.

Phase 1 of the test series consists of two periods of heating, firstly with a constant heat input (varying temperatures) and secondly, after approximately two weeks of ambient cooling, with constant inlet temperature (40 °C). Tests in phase 2 consist of three periods of heating followed by three periods with cooler inlet temperatures reducing to 10 °C inlet temperature in the last of these tests. These tests were also in slightly cooler environmental conditions. During phase 3, the tests were conducted with the lowest inlet temperatures: either 0 °C or -4 °C. This phase of the tests was also during the coldest environmental conditions. The final phase (4) continued after a period of rest with one period of cooling and one period of heating. The range of conditions occurring during the test series accordingly represent a full range of conditions that could be expected in an operating system (probably a little higher and a little lower range of inlet temperatures) including both heating and cooling modes.

The heat transfer fluid used in the tests was a monopropylene glycol and water antifreeze mixture. During the first phases of the test this was at a concentration of 21%. This concentration was increased to 32% at the start of the cooling tests in phase 2 and for the remaining tests. This was to guard against freezing in the same way as often followed in geothermal heating systems. Functions were implemented in the model to calculate glycol thermal properties according to temperature and concentration at each time step using published physical property data

[37]. Examination of the fluid temperatures and flow rates showed that due to the sensitivity and non-linear nature of the properties of the glycol mixture with respect to temperature (particularly variation in viscosity) this results in considerable variation in flow conditions during the test series. In particular, flow in the first series is in the turbulent regime but when the concentration was increased and temperatures approach zero, the fluid became more viscous and the Reynolds Number was calculated to fall into what could be expected to be the laminar regime. The pump flow rate can also seen to diminish as the test series progresses (Fig. 6). Batini et al. [38] have previously commented on up to 11% variation in energy pile heat transfer rates according to glycol concentration but do not consider the variation in properties during operation.

4. Results

4.1. Model validation

As the function of the model is to predict system (pipe) heat transfer rates and outlet temperatures for the purposes of thermal system design, we evaluate the model by considering the errors of prediction of the outlet temperatures and heat transfer rates under a range of conditions. In the validation study, as the pile under test was entirely exposed to the environment at the upper surface we have applied the same environmental boundary conditions (Eq. (14)) to the whole of the upper boundary in the model. We have implemented a general purpose energy pile model that allows for two upper boundary conditions but, for the first phase of validation testing where the whole of the upper surfaces are exposed to the environment, we simply apply the same boundary conditions at both the upper surfaces in the model.

One question that arises in simulating all forms of ground heat exchanger is the choice of initial temperatures. In most models a single temperature is chosen and is often also assumed to be the fixed upper boundary temperature during the whole simulation. This temperature, in the absence of measurements, is often taken to be the mean annual dry-bulb temperature. In reality the ground vertical temperature distribution experienced in pile installations is more variable. Details of the initial ground temperature variations at the test site are reported elsewhere [36]. This could, as a general practice, be calculated using a model such as that by Kasuda and Archenbach and a suitable mean value derived but this is not what was done in this study.

Spatial variations in temperature are not calculated explicitly in a DTN representation. Hence it is not possible to impose a variable temperature gradient at the start of the calculation directly. However, such variations are implicit in the state of the boundary fluxes and the temperature histories used to initialize the model. Hence one approach to arriving at a initial conditions is to use the annual variation in environmental conditions as the upper boundary condition and to simulate the effect of the climate on ground temperatures in the absence of

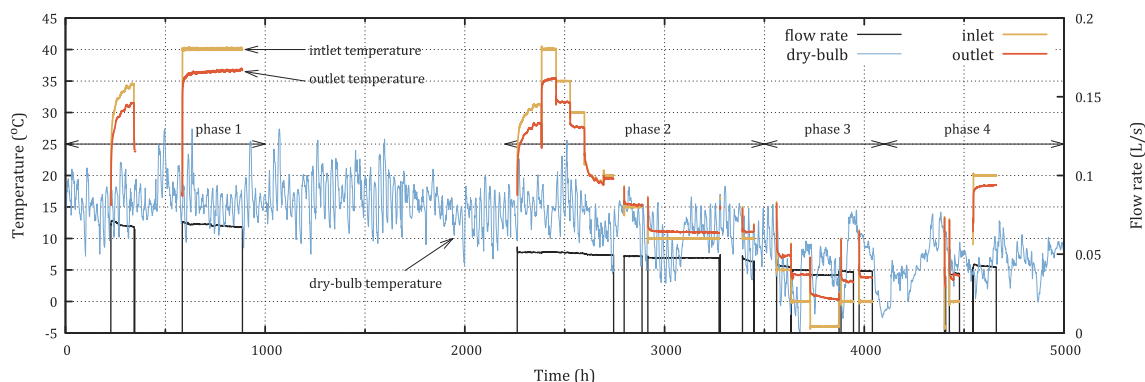


Fig. 6. Thermal response test series conditions.

pile operation i.e. adiabatic conditions at the pipe boundary. This is the approach we propose and have tested in this study. Conducting a number of years of annual simulations of climatic conditions is quite practical as the model is relatively fast to execute. We have also made calculations with a single value for the temperature and upper boundary conditions corresponding to the measured temperature at the start of the test (14.1 °C) and the mean annual dry-bulb temperature (10.1 °C).

Predicted outlet temperatures are compared with measured values during the simulated first phase of tests in Fig. 7. The magnitude of the difference between measured and predicted outlet temperatures are also shown against the righthand axis. The predicted temperatures are in good agreement during both the variable inlet temperature and constant inlet temperature conditions. The difference between the outlet temperatures falls to within the range of experimental temperature measurement error (approximately 0.2 K) for much of the second heating period.

Results for the second phase of testing are shown in Fig. 8. The first tests in heating mode show very similar trends in terms of the differences between predicted and measured outlet temperature as in phase 1. Differences are generally larger during the initial hour of the test when a step change in conditions occurs. A change in fluid properties took place during this phase before the inlet temperature was reduced to 15 and then 10° C and this change in concentration and fluid properties is also represented in the model. The error in outlet temperature prediction is slightly larger in the final test of this phase. This phase also corresponds to a fall in the atmospheric dry-bulb conditions (October and November 2015). It should be noted that these results were obtained with the environmental conditions modelled at the upper boundary throughout the simulated test, including the interval between phase 1 and phase 2. Results assuming fixed initial and upper boundary temperatures gave larger errors.

Results for the third phase of testing are shown in Fig. 9. Inlet temperatures were controlled at 5 °C, 0 °C and -4 °C during these five tests. The response seen in the outlet temperatures during these cooling tests is a little different to that of the earlier tests such that the temperature difference is nearer to being constant but also shows some irregular fluctuations. The model results show a similar form of response to earlier tests but the differences are noticeably larger. The fourth test shows a predicted outlet temperature that increases in the later part of the test and approaches the measured value more closely. This fluctuation can only be induced in the model by the changes in environmental conditions at the upper surface rather than the pipe boundary conditions. It was noted earlier that the fluid flow conditions during the third phase of the test are most likely laminar in nature ($Re < 1000$). The relationship between flow rate and heat transfer effectiveness are highly non-linear in the transition between laminar and fully turbulent flow and notoriously hard to model. If completely laminar conditions are assumed the model predicts very low heat transfer rates.

In the absence of convection coefficient correlations that deal with the whole range of Reynolds Number, we interpolate between the laminar and a lower limit of turbulence value. The model implements a 'smoothstep' (sigmoid) function to achieve this and avoid any discontinuity that could make convergence in dynamic simulation difficult to achieve. The results (Fig. 9) are reasonable under these assumptions. Although the Reynolds Number was found to fall to a low value indicative of laminar flow conditions, given the bends, valves, fittings etc. in the circuit, it is doubtful whether completely laminar conditions would occur. We therefore suggest that both the experimental conditions and the model assumptions in these low temperature (high viscosity), low Reynolds Number conditions are more uncertain than during other tests in the series.

A further assessment of the validity of the model predictions has been made by calculating the Root Mean Square Error (RMSE) of the predicted vs. measured outlet temperature and also the relative error in

the prediction of heat extraction and heat rejection. These values have been calculated using different treatment of the initial and upper surface boundary conditions. Results are presented in Table 3. These values are calculated using data from the whole data set. Using the mean annual temperature as a boundary condition resulted in both over prediction of heat rejection (18.5%) and under prediction (-13.7%) of heat extraction (mostly occurring in phase 3 of the test series). Using a higher value of initial/environmental temperature shifted the balance between predicted heat rejection and extraction such that heat rejection was moderately under-predicted (-5.06%) but heat extraction was noticeably over predicted (25.3%).

The most successful approach was found to be to apply a pre-simulation stage to impose the environmental temperature variation and then to continue simulation of the environmental conditions at the upper boundary during simulation of the energy pile operation. This gave a very modest RMSE of 0.24 K in predicted outlet temperature and relative error in both predicted heat rejection and extraction of better than 4% and we suggest this can be accepted as satisfactory for simulation and design calculation purposes.

4.2. Annual simulation

In order to evaluate the utility of the model as a design tool, and to investigate sensitivity to the treatment of the boundary conditions, a further study was made of the predicted behaviour of the test pile under long-term exposure to thermal loads. This was done using inlet temperatures derived from simulation of a prototypical office building under similar climatic conditions to those at the validation test site. The heating and cooling load variation over the simulated year and the relationship to the dry-bulb temperature are illustrated in Fig. 10. The simulation time step size is fifteen minutes.

A fraction of the total building heating and cooling demand was applied to a pile of the same configuration as the test pile. The proportion applied was adjusted under nominal conditions so that the fluid temperature remained within the bands expected of typical heat pump operation: a maximum of 35° C and minimum of 2° C. The pile is relatively small and this thermal demand corresponded to a maximum system cooling rate (pile heat rejection) of approximately 1.7 kW and system heating rate (heat extraction) of approximately 0.65 kW.

Four variations in treatment of the upper surface boundary conditions have been applied. In general there are two upper surfaces and these are intended to allow representation of the building sub-surface and the exposed ground surrounding the building (see Fig. 2). The combinations of conditions considered are:

1. A fixed upper boundary temperature corresponding to the mean annual air temperature;
2. Simulated environmental conditions over the whole upper surface;

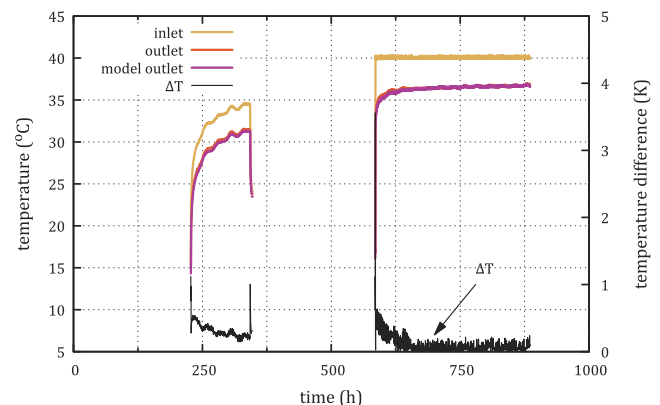


Fig. 7. Measured and simulated thermal response: phase 1 (heat rejection only).

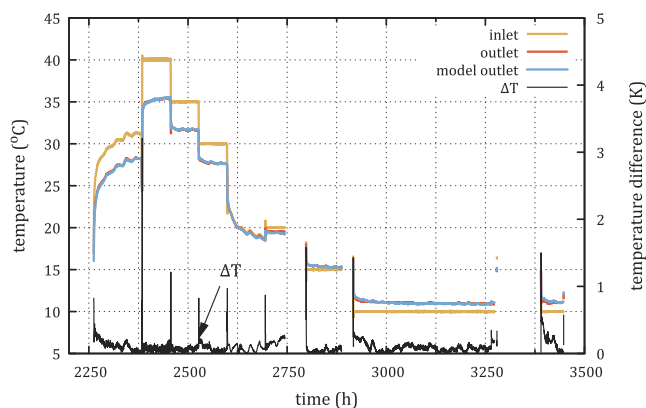


Fig. 8. Measured and simulated thermal response: phase 2 (heating and cooling).

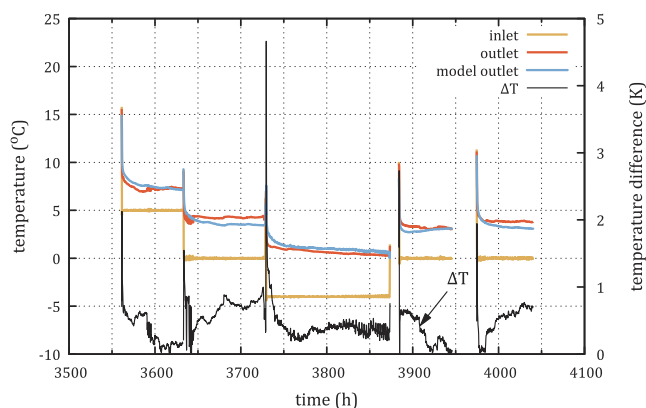


Fig. 9. Measured and simulated thermal response: phase 3 (low temperature heat extraction).

Table 3
Thermal Response Test series prediction errors according to boundary condition treatment.

Surface boundary conditions	Outlet RMSE	Heat rejection	Heat extraction
Fixed (mean average dry-bulb)	0.57 K	18.5%	-13.7%
Fixed (initial measured value)	0.71 K	-5.06%	25.3%
Environmental model	0.24 K	3.62%	3.08%

3. Environmental conditions outside the building and the pile bounding the edge of the building;
4. Environmental conditions outside the building and the pile at the centre of a group under the building.

The first condition is the same as that assumed in many design calculation methods such as those using g-functions [22,14]. The second condition represents the climatic variation in conditions but does not consider the building to have any influence (apart from the system demands) on the thermal conditions experienced by the pile. As the building isolates the head of the pile from the environment to some extent the third condition has the pile exposed to environmental conditions on one side and prototypical building sub-surface conditions on the other i.e. as if the pile were positioned part-way along a building perimeter. The fourth condition has the pile positioned twenty metres from the building perimeter i.e. further isolated from the environment. The building sub-surface is assumed to be an insulated surface with a building above at a constant temperature. This results in a steady heating of the ground sub-surface in this moderate climate i.e. long-term heat losses from the building. Again, we use an implementation of the model that incorporates two upper surfaces and apply the same boundary conditions to both when appropriate (conditions 1 and 2).

These conditions have been simulated by firstly pre-simulating undisturbed ground conditions to reflect the effect of the natural environment. This was followed by simulating the operation of the system over a twenty-five year period (a twenty-five year design calculation period being typical of much design software [14]) and using the arithmetic mean of inlet and outlet temperatures as the main output of interest. Results over the first fifteen years of this period are shown in terms of monthly mean fluid temperatures over repeated annual cycles in Fig. 11. The dominance of the heat rejection (system cooling) demands means that mean fluid temperatures increase over several simulated annual cycles. There is a noticeable difference in temperatures during the first three years of operation. With the first two types of surface boundary condition (denoted ‘constant’ and ‘exposed’ in the plot) the minimum and maximum seasonal temperatures remain nearly constant. The condition where the environment is simulated result in slightly more extreme temperatures than under constant temperature conditions. The differences between conditions continue to grow as the simulation progresses until 25 years.

Where the boundary conditions represent a pile at the edge of the building, both mean monthly minimum and maximum temperatures can be seen to rise over the first five years and then reach a steady-periodic pattern. In the case representing a pile near the centre off the

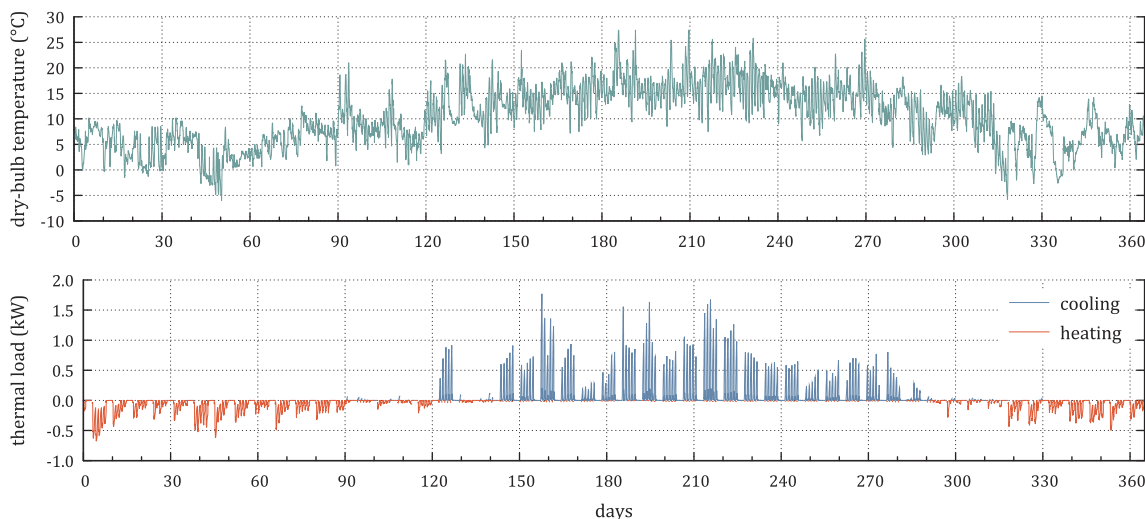


Fig. 10. Simulated thermal loads imposed on the energy pile and corresponding climate data.

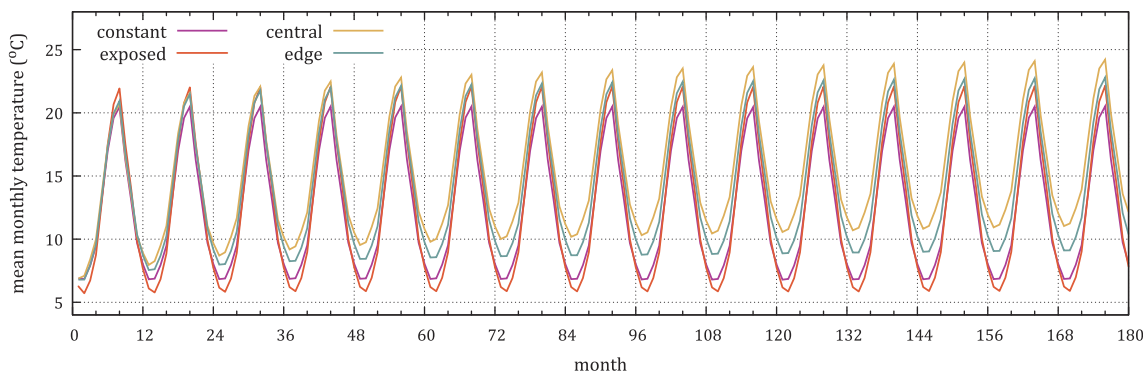


Fig. 11. Predicted monthly mean fluid temperatures over a twenty-five year period with different boundary conditions at the ground surfaces.

installation, the monthly minimum and maximum temperatures continue to rise from one season to the next over the fifteen year period shown.

Daily mean fluid temperatures predicted for the twenty-fifth year are shown in Fig. 12. These daily mean temperatures highlight the differences that could be expected depending on what is assumed about the effect of the building and surrounding ground. The effect of the building is reflected in generally higher fluid temperatures with the pile simulated as located at the edge having lower temperatures than that located centrally. An interesting difference between simulating a fixed boundary temperature compared to simulating exposure to the environment, is that there is some time-shift in terms of when the minimum and maximum temperatures occur. Comparing the two sets of data it can be seen that assuming constant conditions results in mean daily temperatures that are higher than when simulating the environment in the first half of the year, but lower in the second half of the year.

The results of these super-annual simulations indicate the importance of considering the long-term seasonal operation of the system on the thermal state of the pile and the likely operating temperatures and hence efficiency of the system. Simulating conditions over multiple years in this way would not be feasible in design studies using three-dimensional numerical models. In applying this DTN approach each year of simulation was found to require approximately 1.8 s of simulation time on a single 2 GHz Xeon CPU. We conclude this is very reasonable for use in routine design and simulation tasks. The modelling of more complex arrangements of piles (such as irregular groupings) using this model is simply a question of generating a suitable mesh to derive the weighting factors and a parametric mesh generating tool has been developed to enable this. The model could be subsequently used to evaluate long-term temperature and heat flux boundary conditions that could be used in other models of mechanical behaviour.

5. Conclusions

We have presented a model of energy pile thermal response based on a Dynamic Thermal Network approach. This has a number of features that make it well suited to representing energy piles and related foundation heat exchanger elements. In particular, it can represent complex geometries and heterogeneous thermal properties given a suitable model for deriving the weighting factors. In this case we use a finite volume numerical model and parametric grid generation procedures to generate the discrete weighting factors. Our approach has been to allow three boundary conditions to be represented. This has an advantage of being able to represent the effects of the surrounding environment and the building sub-surface to be represented explicitly in addition to the pipes.

Validation of the model has been undertaken using thermal data from a long series of thermal response tests on single pile at a site in Belgium. This has included study of conditions in both summer and winter environments and both heating and cooling fluid temperature conditions. We have found that the model is well able to predict fluid temperatures and heat transfer rates over this range of conditions with a satisfactory level of accuracy.

The validation study highlighted two issues that were important to address to achieve the best results. Firstly, results were somewhat sensitive to the treatment of the upper boundary conditions and best results were found when the environment was simulated over the whole duration of the test series and that the model was pre-conditioned using the environmental time series data to arrive at a reasonable starting condition. Secondly, results were found to be most uncertain in low temperature conditions when the antifreeze fluid mixture was most viscous and the flow regime was likely to be laminar. This issue requires further investigation from both an experimental and modelling point of view. Having said this, it is unlikely that these conditions would occur in practice as a realistic operating system design would be probably designed to operate with a minimum temperature a few degrees above

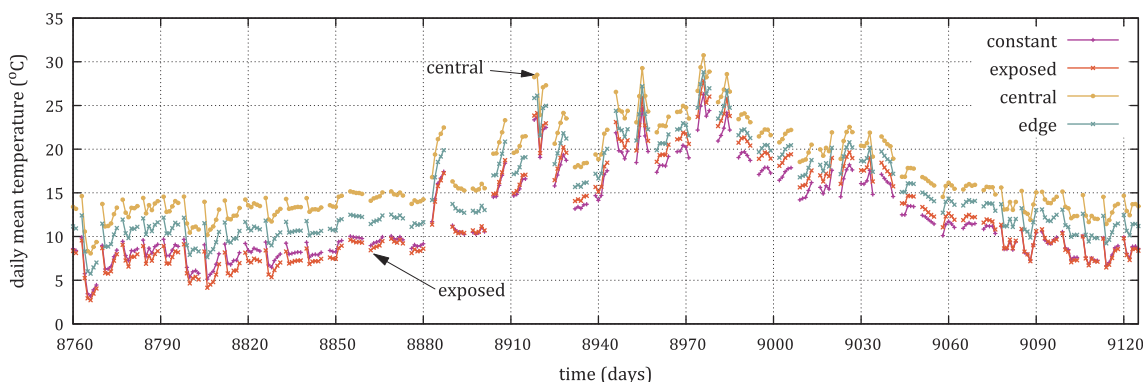


Fig. 12. Predicted daily mean fluid temperatures in the twenty fifth year with different boundary conditions at the ground surfaces.

zero and at a flow rate high enough to ensure fully turbulent conditions.

Simulation of a realistic building heating and cooling demand profile has demonstrated the computational efficiency of the model and highlighted the importance of the boundary conditions at the upper surfaces in energy pile heat exchanger designs. We conclude that it is important to consider the differences in thermal conditions experienced over the long-term by piles positioned at different positions within the array in relation to the edge of the building and the long-term heating effect of the building on the ground below. These effects could be expected to have some impact on the maximum fluid temperatures for a given energy demand and hence long-term efficiency and sustainability. These effects would be in addition to those driven by the grouping of the piles. Differences in the peak temperatures experienced by piles in different positions in the array also suggest different levels of thermal expansion and so potential differential displacements. The choice of boundary conditions used for the inlet conditions and the representation of the building sub-surface conditions and surrounding ground in energy pile design calculations consequently requires further investigation.

Declaration of Competing Interest sections

The authors declare that they have no known competing financial interests or personal relationships that could have appeared to influence the work reported in this paper.

Acknowledgements

Work on model development was made possible thanks to the research project Geothermal Technology for Economic Cooling and Heating, GEOTECH (<http://www.geotech-project.eu>). GEOTECH is co-funded by the European Community Horizon 2020 Program for European Research and Technological Development (2014–2020) and has received research funding from the European Union under grant agreement No. 656889. The experimental campaign was conducted in the framework of the Smart Geotherm research project, funded by the Flemish Agency for Innovation by Science and Technology.

References

- Pérez-Lombard L, Ortiz J, Pout C. A review on buildings energy consumption information. *Energy Build* 2008;40(3):394–8. <https://doi.org/10.1016/J.ENBUILD.2007.03.007>.
- Rees SJ, editor. *Advances in ground source heat pump systems* Oxford: Woodhead Publishing; 2016. <https://doi.org/10.1016/B978-0-08-100311-4.09001-4>.
- Lund JW, Boyd TL. *Direct utilization of geothermal energy 2015 worldwide review. Proceedings of the world geothermal congress 2015, international geothermal association, Melbourne, Australia*. 2015. p. 1–31.
- Adam D, Markiewicz R. Energy from earth-coupled structures, foundations, tunnels and sewers. *Géotechnique*. <https://doi.org/10.1680/geot.2009.59.3.229>.
- Soga K, Rui Y. Energy geostructures. *Adv Ground-Source Heat Pump Syst* 2016;185–221. <https://doi.org/10.1016/B978-0-08-100311-4.00007-8>.
- Brandl H. Energy foundations and other thermo-active ground structures. *Géotechnique* 2006;56(2):81–122. <https://doi.org/10.1680/geot.2006.56.2.81>.
- Pahud D, Dock D, Terminal D, Flughafens E, In VZ. *Measured thermal performances of the Dock Midfield energy pile system at Zürich airport. Proceedings of 9th IEA heat pump conference, 20-22 May, IEA, Zürich, Switzerland*. 2008. p. 1–11.
- Bourne-Webb PJ, Amaty B, Soga K, Amis T, Davidson C, Payne P. *Energy pile test at Lambeth College, London: geotechnical and thermodynamic aspects of pile response to heat cycles*. *Géotechnique* 2009;59(3):237–48. <https://doi.org/10.1680/geot.2009.59.3.237>.
- Garber D. *Ground source heat pump system models in an integrated building and ground energy simulation environment* Ph.D. thesis University of Cambridge; 2013.
- Loveridge FA, Powrie W, Amis T, Wischy M, Kiauk J. Long term monitoring of CFA energy pile schemes in the UK. Aug 2016.
- Abuel-Naga H, Raouf A, Raouf M, Nasser A. Energy piles: current state of knowledge and design challenges. *Environ Geotech* 2014;2. <https://doi.org/10.1680/envgeo.13.00019>.
- Bourne-Webb P, Burlon S, Javed S, Kürten S, Loveridge F. Analysis and design methods for energy geostructures. *Renew Sustain Energy Rev* 2016;65:402–19. <https://doi.org/10.1016/j.rser.2016.06.046>.
- McCartney JS, Sánchez M, Tomac I. Energy geotechnics: Advances in subsurface energy recovery, storage, exchange, and waste management. *Comput Geotech* 2016;75:244–56. <https://doi.org/10.1016/j.compgeo.2016.01.002>.
- Spitler JD, Bernier M. Vertical borehole ground heat exchanger design methods. In: Rees SJ, editor. *Advances in ground-source heat pump systems* (Chapter 2), Woodhead Publishing; 2016. p. 29–61. <https://doi.org/10.1016/B978-0-08-100311-4.00002-9>.
- CIBSE. *Ground source heat pumps: CIBSE TM51*. Chartered Institute of Building Services Engineers, London, UK, 2013.
- Salciarini D, Ronchi F, Tamagnini C. Thermo-hydro-mechanical response of a large piled raft equipped with energy piles: a parametric study. *Acta Geotech* 2017;12(4):703–28. <https://doi.org/10.1007/s11440-017-0551-3>.
- Olgun CG, Ozudogru TY, Abdelaziz SL, Senol A. Long-term performance of heat exchanger piles. *Acta Geotech* 2015;10(5):553–69. <https://doi.org/10.1007/s11440-014-0334-z>.
- Zarella A, De Carli M, Galgaro A. Thermal performance of two types of energy foundation pile: Helical pipe and triple U-tube. *Appl Therm Eng* 2013;61(2):301–10. <https://doi.org/10.1016/j.applthermaleng.2013.08.011>.
- Pahud D, Fromentin A. PILESIM: a simulation tool for pile and borehole heat exchanger systems. *Bulletin d'Hydrologie* 17;1999.
- Hellström G. *Duct ground heat storage model manual*. Tech. Rep., Department of Mathematical Physics, University of Lund, Lund, Sweden, 1989.
- Loveridge F, Powrie W. Temperature response functions (G-functions) for single pile heat exchangers. *Energy* 2013;57:554–64. <https://doi.org/10.1016/j.energy.2013.04.060>.
- Loveridge F, Powrie W. G-Functions for multiple interacting pile heat exchangers. *Energy* 2014;64:747–57. <https://doi.org/10.1016/j.energy.2013.11.014>.
- Makasis N, Narsilio GA, Bidarmaghz A. A robust prediction model approach to energy geo-structure design. *Comput Geotech* 2018;104:140–51. <https://doi.org/10.1016/j.compgeo.2018.08.012>.
- Makasis N, Narsilio GA, Bidarmaghz A. A machine learning approach to energy pile design. *Comput Geotechnics* 2018;97(September 2017):189–203. <https://doi.org/10.1016/j.compgeo.2018.01.011>.
- Rees SJ, Fan D. A numerical implementation of the Dynamic Thermal Network method for long time series simulation of conduction in multi-dimensional non-homogeneous solids. *Int J Heat Mass Transf* 2013;61(6):475–89. <https://doi.org/10.1016/j.ijheatmasstransfer.2013.02.016>.
- Fan D, Rees SJ, Spitler JD. A dynamic thermal network approach to the modelling of Foundation Heat Exchangers. *J Build Performance Simul* 2013;6(2):81–97. <https://doi.org/10.1080/19401493.2012.696144>.
- Claesson J. *Dynamic thermal networks. Outlines of a general theory*. In: *Proceedings of the 6th symposium on building physics in the Nordic countries, Trondheim, Norway, 2002*, p. 47–54.
- Claesson J. *Dynamic thermal networks. Background studies I: elements of a mathematical theory of thermal responses*. Göteborg, Sweden: Chalmers University of Technology, Departmental Report; 2002.
- Claesson J. *Dynamic thermal networks: a methodology to account for time-dependent heat conduction*. In: *Proceedings of the 2nd international conference on research in building physics, Leuven, Belgium, 2003*, p. 407–415.
- Wentzel E-L. *Thermal modeling of walls, foundations and whole buildings using dynamic thermal networks* Ph.D. thesis Göteborg, Sweden: Chalmers University of Technology; 2005.
- Strand RK. *Heat source transfer functions and their application to low temperature radiant heating systems* Ph.D. thesis University of Illinois at Urbana-Champaign; 1995.
- Gnielinski V. New equations for heat and mass transfer in turbulent pipe and channel flow. *Int Chem Eng* 1976;16(2):359–68.
- Serghides TK. Estimate friction factor accurately. *Chem Eng* 1984;91(5):63–4.
- Weller HG, Jasak H, Tabor G. A tensorial approach to computational continuum mechanics using object-oriented techniques. *Comput Phys* 1998;12(6):620–31.
- Van Lysebetten G, Allani M. Real-scale test campaign on energy piles for Belgian practice and numerical modelling of their behaviour. In: *Proceedings of the 19th international conference on soil mechanics and geotechnical engineering, Seoul 2017, Seoul, Korea, 2017*, p. 3475–78.
- Allani M, Van Lysebetten G, Huybrechts N. Experimental and numerical study of the thermo-mechanical behaviour of energy piles for Belgian practice. In: F. A, L.L. editors. *Advances in laboratory testing and modelling of soils and shales (ATMSS)*, Springer, 2017, p. 405–12. https://doi.org/10.1007/978-3-319-52773-4_48.
- ASHRAE. *Physical properties of secondary coolants (brines)*. In: *Ashrae Handbook Fundamentals SI Edition*, American Society of Heating, Refrigerating and Air-Conditioning Engineers, Atlanta, GA, USA, 1997, Ch. 20.
- Batini N, Rotta Loria AF, Conti P, Testi D, Grassi W, Laloui L. Energy and geotechnical behaviour of energy piles for different design solutions. *Appl Therm Eng* 2015;86:199–213. <https://doi.org/10.1016/j.applthermaleng.2015.04.050>.